

1 **Conservation of a DNA replication motif among phylogenetically distant**  
2 **budding yeast species**

3 Haniam Maria<sup>1</sup>, Shivali Kapoor<sup>1</sup>, Tao Liu<sup>2</sup>, and Laura N. Rusche<sup>1\*</sup>

4 <sup>1</sup> Department of Biological Sciences, State University of New York at Buffalo, Buffalo NY, 14260, USA

5 <sup>2</sup> Department of Biostatistics and Bioinformatics, Roswell Park Comprehensive Cancer Center, Buffalo  
6 NY, 14203

7 \*Author for Correspondence: Laura Rusche, Department of Biological Sciences, State University of New  
8 York at Buffalo, Buffalo NY, Telephone: 716-645-5198, Email: [lrusche@buffalo.edu](mailto:lrusche@buffalo.edu)

9      **Abstract**

10        Eukaryotic DNA replication begins at genomic loci termed origins, which are bound by the Origin  
11      Recognition Complex (ORC). Although ORC is conserved across species, the sequence composition of  
12      origins is more varied. In the budding yeast *Saccharomyces cerevisiae*, the ORC binding motif consists of  
13      an A/T-rich 17 bp “extended ACS” sequence adjacent to a B1 element composed of two 3 bp motifs. Similar  
14      sequences occur at origins in closely related species, but it is not clear when this type of replication origin  
15      arose and whether it pre-dated a whole genome duplication that occurred around 100 million years ago in  
16      the budding yeast lineage. To address these questions, we identified the ORC binding sequences in the non-  
17      duplicated species *Torulaspora delbrueckii*. We used chromatin immunoprecipitation followed by  
18      sequencing and identified 190 ORC binding sites distributed across the eight *T. delbrueckii* chromosomes.  
19      Using these sites, we identified an ORC binding motif that is nearly identical to the known motif in *S.*  
20      *cerevisiae*. We also found that the *T. delbrueckii* ORC binding sites function as origins in *T. delbrueckii*  
21      when cloned onto a plasmid and that the motif is required for plasmid replication. Finally, we compared an  
22      *S. cerevisiae* origin with two *T. delbrueckii* ORC-binding sites and found that they conferred similar  
23      stabilities to a plasmid. These results reveal that the ORC-binding motif arose prior to the whole genome  
24      duplication and has been maintained for over 100 million years.

25

26      **Key Words:** autonomously replicating sequence (ARS), ARS consensus sequence (ACS), *Torulaspora*  
27      *delbrueckii*, replication origin, whole genome duplication (WGD), Origin Recognition Complex (ORC)

28 **Significance**

29 DNA replication is the process by which the genome doubles in preparation for cell division. In organisms  
30 such as animals, plants, and fungi, replication starts at multiple locations throughout the genome, ensuring  
31 efficient doubling. These initiation sites are defined differently across species, and in budding yeast, which  
32 are single-celled fungi, a specific DNA sequence is required. This study reveals that this DNA sequence  
33 can be remarkably stable over evolutionary time. We found that the same sequence is used in two yeasts,  
34 *Saccharomyces cerevisiae* and *Torulaspora delbrueckii*, whose last common ancestor existed over 100  
35 million years ago.

36 **Introduction**

37 DNA replication is an essential step in the cell cycle that is required for inheritance of genetic  
38 information. Replication begins at genomic loci termed origins of replication, which are demarcated by the  
39 origin recognition complex (ORC) in eukaryotes. ORC is a six-subunit protein complex that binds directly  
40 to DNA (Bell and Stillman 1992). Although ORC is conserved across eukaryotes, the DNA sequence to  
41 which it binds varies. For example, in the fission yeast *Schizosaccharomyces pombe*, ORC binds stretches  
42 of A/T-rich sequences in a stochastic manner (Dai, et al. 2005; Patel, et al. 2006; Segurado, et al. 2003),  
43 whereas in the budding yeast *Saccharomyces cerevisiae*, ORC binds a specific A/T-rich consensus  
44 sequence (Theis and Newlon 1997). Although this ORC binding motif is conserved among closely related  
45 *Saccharomyces* species (Müller and Nieduszynski 2012), it is not known when it arose or how stable it has  
46 been over evolutionary time.

47 In the budding yeast *S. cerevisiae*, replication origins were initially identified by their ability to  
48 support replication of plasmids and were consequently termed autonomously replicating sequences (ARSs)  
49 (Chan and Tye 1980; Hsiao and Carbon 1979; Struhl, et al. 1979). ARSs in *S. cerevisiae* are characterized  
50 by a 17 bp A/T-rich motif termed the extended ARS Consensus Sequence (ACS) (Theis and Newlon 1997;  
51 Theis, et al. 1999) coupled with an adjacent element termed B1 (Marahrens and Stillman 1992). The entire  
52 consensus sequence spans 33 bp and is termed the ORC-ACS (Eaton, et al. 2010; Xu, et al. 2006). Among  
53 other related yeast species whose origins have been examined, *Candida glabrata* has a 17 bp extended ACS  
54 similar to that of *S. cerevisiae* and a weak signature of the B1 element (Descorps-Declère, et al. 2015). In  
55 contrast, the more evolutionarily distant budding yeast species *Lachancea kluyveri* and *Lachancea waltii*  
56 have similar but shorter ACS-like elements, and a B1 element with a different consensus sequence (Di  
57 Rienzi, et al. 2012; Liachko, et al. 2011). Another budding yeast, *Kluyveromyces lactis*, has considerably  
58 different origins, with an unusually long 50 bp ACS composed of short patches of A/T nucleotides  
59 (Liachko, et al. 2010). However, the evolutionary distance between these species and *S. cerevisiae* limits  
60 our understanding of how and when replication origins have evolved. To enhance evolutionary

61 comparisons, we have now identified ORC binding sites in a budding yeast species, *Torulaspora*  
62 *delbrueckii*, that belongs to a lineage of budding yeast species whose origins of replication have not been  
63 explored (Figure 1A).

64 *T. delbrueckii*, like *Lachancea* and *Kluyveromyces* species, diverged from *Saccharomyces* species  
65 before a whole genome duplication (Shen, et al. 2018). This duplication is thought to have occurred more  
66 than 100 million years ago through the hybridization of two yeast species -- one from the  
67 *Zygosaccharomyces* and *Torulaspora* (ZT) clade, to which *T. delbrueckii* belongs, and one from the  
68 *Kluyveromyces*, *Lachancea*, and *Eremothecium* (KLE) clade (Marcel-Houben and Gabaldon 2015).  
69 Although the doubled genome originally had equal portions from the two parents, subsequent  
70 pseudogenization and gene loss was biased, such that duplicated species like *S. cerevisiae* retain more genes  
71 from the ZT lineage than the KLE lineage (Marcel-Houben and Gabaldon 2015). Although replication  
72 origins have been identified in species from the KLE clade, origins have not been studied in any species  
73 from the ZT clade. Identifying the origins in both parental lineages involved in the ancient hybridization  
74 will improve our understanding of how origin selection was affected by this event.

75 A good proxy for the locations of origins are the ORC binding sites because DNA replication  
76 begins with the ATP-dependent binding of ORC to the origin DNA. Therefore, to determine the locations  
77 of origins of replication throughout the *T. delbrueckii* genome, we coupled chromatin immunoprecipitation  
78 of three subunits of the ORC complex with high throughput DNA sequencing. We identified 190 ORC  
79 binding sites across the eight chromosomes in the *T. delbrueckii* genome. We then used these 190 sequences  
80 to predict an ORC binding motif. We identified a conserved motif that is strikingly similar to the *S.*  
81 *cerevisiae* ORC-ACS. We further found that several representative ORC binding sites function as ARSs  
82 when placed on a plasmid and that the conserved motif is required for this ARS function. Finally, we  
83 compared the stabilities of plasmids bearing an *S. cerevisiae* origin and two *T. delbrueckii* ORC-binding  
84 sites and found that they were similar. Overall, this study reveals that the consensus sequence that supports  
85 ORC binding and DNA replication in *S. cerevisiae* pre-dates the whole genome duplication and was likely  
86 contributed by one of the two parents.

87 **Results**

88 **Identification of *T. delbrueckii* ORC binding sites.** In eukaryotes, the first step of DNA replication is  
89 ATP-dependent association of the six-subunit origin recognition complex (ORC) with chromosomal  
90 replication origins. To identify regions of the *T. delbrueckii* genome that are potential replication origins,  
91 we mapped ORC binding sites across the genome using chromatin immunoprecipitation followed by high  
92 throughput sequencing (ChIP-Seq). We immunoprecipitated chromatin fragments associated with three  
93 epitope tagged subunits of the ORC complex, Orc1, Orc2 and Orc4 (Figure 1B). Orc1 had a 3XMYC  
94 epitope tag, whereas Orc2 and Orc4 had V5 epitope tags. Using two different tags could reduce false signal  
95 due to non-specific immunoprecipitation. We also included a mock immunoprecipitation from an untagged  
96 strain. Sequence reads from each ChIP sample were aligned to the *T. delbrueckii* genome (Figure 1C), and  
97 then one million randomly selected high quality reads were used to identify sites of higher enrichment  
98 (peaks) using MACS2 (Zhang, et al. 2008). We identified a total of 216 Orc1 binding sites, 264 Orc2  
99 binding sites and 227 Orc4 binding sites that were present in replicate ChIP-Seq samples from two  
100 independently tagged strains for each subunit (Supplemental Figure 1). Finally, we identified 190 sites  
101 associated with all three ORC subunits (Figure 1D). These ORC binding sites averaged 670 bp in length  
102 and had p-values of  $10^{-3}$  or better (Supplemental Table 1). Binding sites were named systematically based  
103 on their location, including the chromosome number and linear coordinate divided by 1000.

104

105 **Locations of *T. delbrueckii* ORC binding sites.** The genome of *T. delbrueckii* is ~9.22 Mb and is  
106 distributed across eight chromosomes with 4,972 open reading frames (ORFs) (Gomez-Angulo, et al. 2015;  
107 Gordon, et al. 2011). To determine how replication origins are distributed across the genome, we plotted  
108 the positions of the 190 *T. delbrueckii* ORC binding sites (Figure 2, Supplemental Figure 2). As described  
109 in more detail below, most ORC binding sites were intergenic. The average distance between sites was 47  
110 kbp. We also examined the proximity of ORC binding sites to features reported to be near origins in other  
111 yeast. Specifically, centromeres (Descorps-Declère, et al. 2015; Di Rienzi, et al. 2012; Koren, et al. 2011;

112 Müller and Nieduszynski 2017) and histone genes (Müller and Nieduszynski 2017; Raghuraman, et al.  
113 2001) replicate early in other yeast species. Seven of the eight *T. delbrueckii* centromeres are within 11.4  
114 kbp of an ORC binding site, and *CEN8* is 23.6 kbp away. The histone genes are an average of 3.5 kbp and  
115 no more than 9.8 kbp from an ORC binding site.

116

117 **Identification of motif associated with *T. delbrueckii* ORC binding sites.** Origins of replication in *S.*  
118 *cerevisiae* and other budding yeast contain a consensus sequence that is essential for ORC binding and  
119 origin function. In *S. cerevisiae*, the core 11 bp sequence is termed the ACS (ARS (Autonomously  
120 Replicating Sequence) Consensus Sequence) (Theis and Newlon 1997; Theis, et al. 1999), and the full 33  
121 bp sequence is the ORC-ACS (Eaton, et al. 2010; Xu, et al. 2006). To identify a functionally similar  
122 sequence required for ORC binding in *T. delbrueckii*, we searched for a consensus motif among the 190  
123 ORC binding sites identified by ChIP-Seq. We first used the motif finder MEME (Bailey, et al. 2009)  
124 without specifying the motif length and obtained a 17 bp conserved motif that was present in 187 of 190  
125 ORC binding sequences (Figure 3A). Interestingly, this motif is nearly identical to the published extended  
126 ACS for *S. cerevisiae* and *C. glabrata* (Descorts-Declère, et al. 2015; Eaton, et al. 2010) but less similar to  
127 motifs from non-duplicated yeast in the KLE clade (Figure 3B). For example, *L. kluyveri*, has a shorter 9  
128 bp ACS (Liachko, et al. 2011), and *L. waltii* has a 13 bp ACS (Di Rienzi, et al. 2012).

129 We next fixed the motif length to 33 bp to investigate if there is a B1-like element in *T. delbrueckii*,  
130 as in *S. cerevisiae*. Indeed, when a longer motif was specified, MEME returned a sequence that included  
131 the extended ACS as well as two shorter motifs resembling the *S. cerevisiae* B1 element (Figure 3B). This  
132 motif occurred in 188 of the 190 ORC binding sites when a first order Markov model of the background  
133 was built. One binding site, TdARS\_VI\_530, did not have a match to the consensus motif in this analysis,  
134 but did have a match when a second order Markov model of the background was built. For another binding  
135 site, III\_1257, no match to the conserved motif was detected, although inspection of the genome browser  
136 indicated that ORC was associated with this site (Supplemental Figure 4A). As described below, this site  
137 had low replication activity on a plasmid. Overall, the motif we detected was more similar to the *S.*

138 *cerevisiae* ORC-ACS than motifs described in non-duplicated species from the KLE clade. In these species,  
139 the consensus sequence of the B1 element is longer than in *S. cerevisiae* and *T. delbrueckii*. In contrast, the  
140 duplicated species *C. glabrata* has a weak match to the B1 element (Descorts-Declère, et al. 2015). Thus,  
141 the motif associated with *T. delbrueckii* ORC binding sites is highly similar to the ORC-ACS motif known  
142 in *S. cerevisiae*, suggesting that this sequence arose in a common ancestor of the two species and prior to  
143 the genome duplication.

144

145 **A tyrosine in Orc4 that contacts DNA is found in species with an extended ACS.** Cryo-EM studies of  
146 the *S. cerevisiae* pre-replication complex indicate that a loop in Orc2 and an alpha-helix in Orc4 make direct  
147 contacts with DNA in the extended ACS (Yuan, et al. 2017). Moreover, genetic studies pinpoint tyrosine  
148 486 in ScOrc4 as conferring specificity for nucleotides 14 and 15 in the ACS (Hu, et al. 2020). These  
149 positions harbor A/T and G/T in *S. cerevisiae*, *C. glabrata*, and *T. delbrueckii*, but no particular nucleotide  
150 is found at these positions in the KLE ORC binding sites (Figure 3B). To determine whether having defined  
151 nucleotides at these positions within the ORC binding motif (Figure 3B: red boxed nucleotides (*S.*  
152 *cerevisiae* positions 14 and 15 and *T. delbrueckii* positions 12 and 13)) correlates with the presence of this  
153 tyrosine, we aligned the Orc4 sequences from the same species (Figure 3C). Indeed, the tyrosine residue  
154 occurred in *S. cerevisiae*, *C. glabrata*, and *T. delbrueckii* but not in the KLE species.

155

156 **ORC binding motifs coincided with the peak of ORC enrichment.** If the ACS-like motif we detected  
157 by MEME is the ORC recognition site, it should coincide with the peak of ORC binding at each site. We  
158 therefore generated aggregate plots and heat maps of the ChIP-Seq signals from the three ORC subunits  
159 centered around the 33 bp motif (Figure 4C). For this analysis, the motifs were all oriented the same way.  
160 As predicted, the peak of ORC binding did coincide with the motif. Interestingly, we observed that the  
161 maximum enrichment was at slightly different positions for the three subunits. The peak for Orc1 was ~60  
162 bp upstream of the center of the motif (nucleotide 17), for Orc4 it was ~20 bp upstream, and for Orc2 it was  
163 ~10 bp downstream of the center of the motif. This result is consistent with crosslinking studies of *S.*

164 *cerevisiae* ORC that show a differential arrangement of the ORC subunits across the ACS (Lee and Bell  
165 1997).

166

167 ***T. delbrueckii* ORC binding motifs were preferentially located in intergenic regions.** In other yeasts,  
168 replication origins are primarily located in intergenic regions (Descorts-Declère, et al. 2015; Di Rienzi, et  
169 al. 2012; Liachko, et al. 2010; Nieduszynski, et al. 2007). To determine if this is also true in *T. delbrueckii*,  
170 we determined the positions of the 189 ORC binding motifs relative to the flanking genes. We found a  
171 strong preference for intergenic regions, with 170 of 189 motifs (90%) located within an intergenic region  
172 (Figure 4A). The average length of these 170 intergenic regions was 784 bp. In contrast, intergenic regions  
173 without an ORC binding site were shorter, with an average length of 357 bp (Figure 4B). We also examined  
174 the orientations of the genes flanking intergenic regions with ORC binding sites (Figure 4A). There was a  
175 slight bias for ORC-binding motifs to be positioned with one gene transcribing towards the motif and the  
176 other transcribing away from it. This arrangement was observed for 98 out of 170 motifs (57.6%), which is  
177 slightly higher than the 50% expected with no bias. Approximately equal numbers of motifs were located  
178 between divergently transcribed genes (37) and convergently transcribing genes (34). Thus, most of the *T.*  
179 *delbrueckii* ORC-binding sites are located within intergenic regions, where they are less likely to interfere  
180 with transcription, but there is no favored orientation of the flanking genes.

181

182 **ORC binding sites enabled plasmids to replicate.** An autonomously replicating sequence (ARS) is a  
183 sequence that is sufficient to allow a plasmid to replicate. To test whether the *T. delbrueckii* ORC binding  
184 sites are functional ARSs, we cloned six representative binding sites into a plasmid lacking an origin and  
185 assessed whether the plasmid was stable in *T. delbrueckii*. These six ORC binding sites (TdARS\_VII\_22,  
186 69, 228, 525, 681, and 734) were 330 to 580 bp in length, and each had a fold enrichment of three or more  
187 for all three ORC subunits (Figure 5). We focused on ORC binding sites on chromosome VII because we  
188 wanted to identify ORC-binding sites adjacent to the cryptic mating type locus *HMRa1* (unpublished data).  
189 The ORC binding sites were cloned onto a plasmid with no other origin sequences, a hygromycin

190 (antibiotic) resistance gene, and a *T. delbrueckii* centromere to ensure segregation. We also created a similar  
191 plasmid containing *S. cerevisiae* ARS209, which is known to have ARS activity in *T. delbrueckii* (Ellahi  
192 and Rine 2016). Once plasmids were taken up by *T. delbrueckii* cells, efficient replication was required for  
193 growth on medium with hygromycin; therefore, only plasmids bearing a functional ARS yielded robust  
194 colonies (Figure 6A). We observed that all six ORC binding sites had strong ARS function, producing  
195 robust colonies similar to those produced with the *S. cerevisiae* ARS. In contrast, a control plasmid lacking  
196 an ORC binding site produced only tiny colonies. To quantify this difference, we measured the average  
197 colony area (Figure 6B) and found that colonies produced with plasmids containing strong ORC binding  
198 sites were  $\geq 1 \text{ mm}^2$ , whereas the control plasmid yielded colonies of less than  $0.09 \text{ mm}^2$ .

199

200 **Conserved motif associated with ORC-binding sites was required for ARS activity.** In *S. cerevisiae*  
201 and other yeast, the ACS is required for ARS activity. To determine whether the motif we detected using  
202 MEME behaves as an ACS, we deleted the consensus sequence from TdARS\_VII\_681, generating  
203 TdARS\_VII\_681 $\Delta$  (Figure 5B). Plasmids carrying this modified ORC binding site produced only tiny  
204 colonies, significantly smaller than those colonies harboring the plasmid with an intact motif (Figure 6A,  
205 B). We also tested the one ORC-binding site that did not have a match to the consensus motif in our MEME  
206 analysis, site III\_1257. All three ORC subunits were present at position III\_1257 (Supplemental Figure  
207 4A). However, plasmids carrying site III\_1257 produced significantly smaller colonies compared to  
208 plasmids bearing an ORC-binding site with the motif (Supplemental Figures 4B and 4C). These findings  
209 indicate that the detected motif is required for replication and therefore behaves as an ACS.

210

211 **Sequences matching the ACS but lacking ORC binding had no ARS activity.** Although the ACS is  
212 required for DNA replication in *S. cerevisiae* and other yeasts, it is not sufficient for origin activity. In fact,  
213 the *S. cerevisiae* genome contains many more matches to the ACS than ORC binding sites or functional  
214 replication origins (Belsky, et al. 2015). This observation prompted us to test whether sequences that match  
215 the ACS motif but lack ORC binding would display ARS activity. To do so, we cloned three genetic loci

216 with potential ACSs but low or questionable ORC enrichment. One site, VII\_55, had a match to the ORC-  
217 binding motif using FIMO (Bailey, et al. 2009), but no ORC enrichment. Another site, VII\_591, had low  
218 enrichment ( $\leq 3$ ) of Orc2 and no enrichment for Orc1 and Orc4. A third site, VII\_6, was subtelomeric and  
219 had a broad peak of Orc1 that likely reflects sub-telomeric heterochromatin. However, Orc2 and Orc4 had  
220 a different pattern of association, with narrow peaks of low enrichment ( $\leq 3$ ) (Supplemental Figure 3). To  
221 determine whether VII\_6 represents a subtelomeric origin, we included it in the ARS assay. Plasmids  
222 containing the three ACS-like sequences produced only tiny colonies with an average area of less than 0.09  
223 mm<sup>2</sup> (Figures 6A and B). This finding indicates that the identified ACS motif alone is not sufficient for  
224 replication and that additional features are needed to recruit ORC and promote DNA replication.

225

226 **Plasmids bearing *S. cerevisiae* and *T. delbrueckii* ARSs were lost at similar rates in *T. delbrueckii*.** The  
227 predicted *T. delbrueckii* ACS is similar to, but not exactly the same as, the *S. cerevisiae* ACS (Figure 3),  
228 which could indicate slight differences in the specificity of ORC in the two species. To compare the abilities  
229 of ScARS209 and *T. delbrueckii* origins to promote replication, we used a plasmid loss assay (Marahrens  
230 and Stillman 1992), which is more sensitive than the transformation assay. We compared the relative  
231 stabilities of plasmids bearing TdARS\_VII\_228 and TdARS\_VII\_681, which have high fold-enrichment  
232 of ORC subunits (Figure 5B), with a plasmid bearing ScARS209. To measure the retention of the plasmid,  
233 yeast containing plasmids were grown for ~15 generations in non-selective medium (YPD), and the fraction  
234 of hygromycin-resistant cells was calculated at the start and end of the non-selective growth. Both the *T.*  
235 *delbrueckii* and the *S. cerevisiae* ARS-containing plasmids showed a similar extent of plasmid loss (Figure  
236 6C), consistent with the sequence features necessary for origin function being similar in the two species.  
237 As an aside, we note that the loss rate for the plasmid we used in *T. delbrueckii* is higher than for the  
238 plasmids that have been studied in *S. cerevisiae* (Marahrens and Stillman 1992). This higher loss rate could  
239 be due to differences in centromere-mediated segregation.

240

241 **Discussion**

242 In this study, we mapped ORC binding sites and characterized their consensus sequences in the  
243 non-duplicated budding yeast *Torulaspora delbrueckii*. Using ChIP-Seq, we identified binding sites for  
244 three of the six subunits of the origin recognition complex (ORC). Out of the 216 Orc1, 264 Orc2 and 227  
245 Orc4 binding sites, 190 sites were associated with all three subunits. We also found a consensus motif in  
246 189 of the 190 ORC binding sites. In addition, we found that six of six tested ORC binding sites with a  
247 consensus motif had autonomous replication function on a plasmid, supporting the expectation that the  
248 ORC binding sites are genomic origins of replication.

249 Our approach of using ChIP-Seq to identify potential origins of replication was less labor-intensive  
250 than screening genomic libraries for ARS activity and homed in on consensus sequences more precisely  
251 than measuring replication timing across the genome. This ChIP-Seq strategy takes advantage of the  
252 foundational role of ORC in recruiting other proteins to the pre-replication complex. In addition, we used  
253 two different epitope tags to reduce technical biases. Validating this approach, all six ORC binding sites  
254 tested for ARS function supported plasmid replication. In contrast, sites that matched the consensus  
255 sequence but had low or no association of the three subunits showed no ARS function. For example, VII\_55,  
256 had a match to the ORC-binding motif but no ORC enrichment, consequently, had no replication function  
257 on a plasmid.

258 The locations of ORC-binding sites across the *T. delbrueckii* genome are consistent with  
259 observations in previously studied budding yeasts. For example, in many yeast species, centromeres and  
260 histone genes replicate early and hence are near origins (Descorps-Declère, et al. 2015; Di Rienzi, et al.  
261 2012; Koren, et al. 2011; Müller and Nieduszynski 2017). Early replication of the centromeres may promote  
262 kinetochore assembly or proper orientation of sister chromatids (McCarroll and Fangman 1988). Similarly,  
263 early replication of histone genes may enhance production of histones prior to duplication of the remaining  
264 genome (Mei, et al. 2017). Consistent with observations in other yeast, we found that *T. delbrueckii* ORC  
265 binding sites are close to centromeres and histone genes. Each of the two copies of histone H2A, H2B, H3,

266 and H4 genes are located within 9.8 kbp of ORC binding sites. Similarly, seven of the eight *T. delbrueckii*  
267 centromeres were within 11.4 kbp of an ORC binding site. *CEN8* is farther from the nearest ORC binding  
268 site (23.6 kbp). An examination of the ChIP-Seq read depth in the vicinity of *CEN8* did not reveal an ORC  
269 binding site that had been missed. Thus, it is either not essential for centromeres to be close to origins, or  
270 *CEN8*, which has not been examined functionally, may not be the actual centromere. Although our work  
271 did not explicitly examine replication timing, these findings are consistent with the importance of early  
272 replication for centromere and histone gene function.

273 The average distance between adjacent ORC binding sites in the *T. delbrueckii* genome is  
274 approximately 47 kbp, which falls in the middle of the range for budding yeasts. The average distance is  
275 shorter for the 269 origins in *S. cerevisiae* (30 kbp), longer for the 124 origins in *K. lactis* (70 kbp), but  
276 about the same for the 195 origins in *L. waltii* (52 kbp) and the 275 origins in *C. glabrata* (45 kbp).  
277 Interestingly, we identified fewer ORC binding sites in *T. delbrueckii* (190) than there are in *S. cerevisiae*  
278 (269). Given that only a fraction of origins are used in any given cell division in *S. cerevisiae* (Friedman,  
279 et al. 1997), it would be interesting to explore the fraction of active origins and replicon size in *T.*  
280 *delbrueckii*. Alternatively, the difference in origin number and spacing may indicate that additional origins  
281 are yet to be discovered in *T. delbrueckii*, which has not been as extensively studied as *S. cerevisiae*.

282 We also found that a majority (90%) of the *T. delbrueckii* ORC-binding sites occur in intergenic  
283 regions, although there was no bias for a particular orientation of flanking genes. This lack of bias is similar  
284 to the non-duplicated species *K. lactis* (Liachko, et al. 2010), but different from *S. cerevisiae* (Nieduszynski,  
285 et al. 2007) and *L. waltii* (Di Rienzi, et al. 2012) where ARSs are biased for intergenic regions between  
286 convergently and divergently transcribed genes, respectively. We also found that intergenic regions with  
287 ORC-binding sites are slightly larger than those without. This arrangement could favor replication initiation  
288 by reducing transcription interference with ORC binding.

289 We noticed in aggregate plots that the peaks of the three ORC subunits were slightly offset from  
290 one another with respect to the consensus motif. The peak of Orc1 was the most 5' relative to the T-rich  
291 strand, and Orc2 was the most 3'. This offset binding is similar to previously reported crosslinking positions

292 (Lee and Bell 1997). Moreover, it is possible that Orc1 contacts DNA upstream of the ORC-ACS motif  
293 through its nucleosome-binding BAH domain. However, the shifted peak of Orc1 could also be a technical  
294 artifact, as the Orc1 ChIP-Seq data was collected at a different time using a different antibody. In addition,  
295 single-end sequencing was used for Orc1 and paired-end sequencing was used Orc2 and Orc4. Therefore,  
296 whether the skewed enrichment of the three ORC subunits is a functional aspect of ORC-DNA interaction  
297 requires further investigation.

298 The consensus sequence we found to be associated with ORC binding sites was essential but not  
299 sufficient for replication of a plasmid. In the ARS assay, deletion of the 17 bp ACS-like motif resulted in  
300 small colony sizes, reflecting little replication of the plasmid. Additionally, an ORC binding site which had  
301 no consensus ORC binding motif replicated poorly. On the other hand, matches to the 17 bp consensus  
302 sequence that were not occupied by ORC produced only tiny colonies, indicating poor or no ARS function.  
303 Hence, there are most likely additional features beyond the consensus motif that are important for ORC  
304 binding and DNA replication. In *S. cerevisiae*, additional B elements downstream of the ORC-ACS are  
305 required for origin function. For example, A-rich B2 elements facilitate helicase loading and unwinding  
306 (Lipford and Bell 2001; Zou and Stillman 2000), and the B3 element recruits Abf1, thereby positioning  
307 nucleosomes (Lipford and Bell 2001). Presumably, similar sequences exist near ORC binding sites in *T.*  
308 *delbrueckii*.

309 Although specific sequences define replication origins in all Saccharomycetaceae yeasts that have  
310 been examined, the consensus sequence varies across species. This variability is particularly pronounced  
311 among the non-duplicated yeast from the *Kluyveromyces*, *Lachancea*, *Eremothecium* (KLE) clade. A  
312 comparative study of ten *Lachancea* species revealed a variety of motifs at replication origins (Agier, et al.  
313 2018), and *K. lactis* has an unusually long 50 bp ARS which barely resembles the consensus motifs from  
314 other budding yeast (Liachko, et al. 2010). In contrast *T. delbrueckii*, belonging to the *Zygosaccharomyces*,  
315 *Torulaspora* (ZT) clade, has a motif that is highly similar to the ORC-ACS found in duplicated species  
316 such as *S. cerevisiae* and *C. glabrata*. We also observed that an *S. cerevisiae* origin and two *T. delbrueckii*  
317 origins confer similar stability to a plasmid in *T. delbrueckii* cells. It is striking that the ORC-ACS motif is

318 so similar in *T. delbrueckii* and *S. cerevisiae*, which diverged over 100 million years ago, whereas origin  
319 motifs have shifted on a shorter time scale among KLE species.

320 The similarity between the ORC-ACS motifs in *S. cerevisiae* and *T. delbrueckii* raises questions  
321 about the early events in the whole genome duplication. In the initial hybridization event, it seems likely  
322 that the ZT parent contributed replication origins of the ORC-ACS type, whereas the KLE parent  
323 contributed another type of origin. Did having two different mechanisms for recognizing origins lead to  
324 genomic instability? How was this conflict ultimately resolved in favor of the ORC-ACS type of origin?  
325 One possibility is that ORC subunits from the ZT parent were retained, favoring use of the ORC-ACS  
326 sequence. Once the ORC proteins favored the ORC-ACS type of origin, DNA derived from the KLE parent  
327 may have been replicated less efficiently than DNA derived from the ZT parent. Did this poor replication  
328 mimic DNA damage and trigger recombination between the homologous KLE and ZT sequences? Did this  
329 lead to loss of heterozygosity in favor of the efficiently replicated ZT sequences? If so, this uneven  
330 replication may have contributed to duplicated species retaining more genetic material from the ZT parent  
331 compared to the KLE parent (Marcet-Houben and Gabaldon 2015).

332 In summary, this work reveals that origin sequences can be stable over long periods of evolutionary  
333 time and sets the stage for future studies on how origin selection mechanisms impact DNA retention after  
334 hybridization events.

335 **Materials and Methods**

336 **Tree construction**

337 To construct the species tree, we selected 10 protein-coding genes (Supplemental Table 2) found  
338 in single copy across the 9 species considered (Aguileta, et al. 2008). Their amino acid sequences were  
339 obtained from the yeast gene order browser (Byrne and Wolfe 2005) and the candida gene order browser  
340 (Maguire, et al. 2013) and then concatenated, resulting in a combined alignment of 9925 positions. The  
341 concatenated sequences were aligned in MAFFT v7.475 using E-INS-i with default settings (Katoh and  
342 Standley 2013). MAFFT alignment was input into IQTree (Trifinopoulos, et al. 2016) to determine the best  
343 amino acid substitution model: LG+F+I+G4 (Hoang, et al. 2018). Finally, a maximum likelihood  
344 phylogenetic tree was constructed using PhyML v3.1 using the LG+F+I+G4 model as implemented in  
345 Seaview v5.0.4 (Gouy, et al. 2010). Node support was assessed with approximate likelihood ratio tests  
346 (aLRT). Subtree pruning and regrafting (SPR) was used as a search algorithm with five random starts.

347

348 **Yeast growth and transformation**

349 Yeast strains used in this study (Supplemental Table 3) were derived from JRY10156 (Ellahi and  
350 Rine 2016), a *Torulaspora delbrueckii* MAT $\alpha$  *ura3Δ0 trp3-1* strain descended from NRRL Y-866. Yeast  
351 were grown at 30°C in YPD medium containing 1% yeast extract, 2% peptone, and 2% glucose. *T.*  
352 *delbrueckii* cells were transformed using electroporation (Hickman and Rusche 2009). Briefly, cells were  
353 harvested at an optical density (OD<sub>600</sub>) ~1 and resuspended at 15 OD/ml in YPD containing 25 mM DTT  
354 and 20 mM HEPES, pH 8. Cells were shaken for 30 minutes at 30°, collected, and washed in electroporation  
355 buffer (10 mM tris pH 7.5, 270 mM sucrose, 1 mM LiOAc). Cells were then resuspended at 100 OD/ml in  
356 electroporation buffer. Electroporation was conducted in 0.2 mm cuvettes using 50  $\mu$ L cells at 1000 V, 300  
357  $\Omega$ , and 25  $\mu$ F. After electroporation, cells recovered 15 minutes in chilled YPD and then three hours at 30°  
358 before plating on selective medium (YPD containing 400  $\mu$ g/mL hygromycin). For strain construction, 100  
359 ng of linear DNA and 1  $\mu$ L of 10 mg/mL sheared salmon sperm DNA (AM9680, Invitrogen) were used in

360 a volume no more than 5  $\mu$ L. For the transformation frequency assay (Clyne and Kelly 1997), JRY10156  
361 was transformed with 5 ng of each plasmid to be tested.

362

### 363 **Plasmid and yeast strain construction**

364 Plasmids used in this study are listed in Supplemental Tables 4 and 5. Plasmids for tagging ORC  
365 subunits were derived from pRS414 (Sikorski and Hieter 1989). *T. delbrueckii* *ORC1* (*TDEL0D00910*),  
366 *ORC2* (*TDEL0D03510*), and *ORC4* (*TDEL0H00550*) reading frames along with ~500 bp flanking sequence  
367 were amplified from genomic DNA (JRY10156) and ligated into pRS414. To tag Orc2 and Orc4, the V5  
368 epitope tag and hygromycin resistance marker were amplified from plasmid pFA6a-6xGLY-V5-hphMX4  
369 (Funakoshi and Hochstrasser 2009) and stitched into the 3' end of each gene. For Orc1, the 3XMYC tag  
370 was inserted in the linker between the BAH and AAA+ domains, and the hygromycin resistance marker  
371 was added downstream of the gene. The 3XMYC epitope tag was amplified from plasmid pWZV87 (Brand,  
372 et al. 1985), and the hygromycin resistance gene was amplified from pFA6a-6xGLY-V5-hphMX4  
373 (Funakoshi and Hochstrasser 2009). To integrate Orc1-3XMYC, Orc2-V5, and Orc4-V5 into *T. delbrueckii*,  
374 tagging constructs were excised from the plasmids by restriction digestion and used to transform JRY10156  
375 (Ellahi and Rine 2016). To confirm an intact reading frame, the tagged genes were sequenced, and to  
376 confirm protein expression, immunoblots were used.

377 Plasmids for the transformation frequency assay were derived from pRS41H (Ellahi and Rine  
378 2016), which has a *T. delbrueckii* centromere (*CEN3*), an *S. cerevisiae* origin (ARS209), and a hygromycin  
379 resistance gene. To facilitate insertion of potential origins, the *S. cerevisiae* ARS was deleted and replaced  
380 with SphI and NheI cut sites, generating pLR1275. Next, ORC binding sites to be tested for ARS activity  
381 were amplified from *T. delbrueckii* genomic DNA (JRY10156) using primers with flanking SphI and NheI  
382 sites. *S. cerevisiae* ARS209 was also amplified from pRS41H using primers with flanking SphI and NheI  
383 sites. III\_1257 was amplified using primers with flanking SphI and XbaI sites. Digested PCR products were  
384 ligated into plasmid pLR1275 using NEB instant sticky-end ligase master mix (NEB M0370S).

385 Additionally, the 17 bp ORC binding motif was deleted from pLR1278 and replaced with XbaI cut site  
386 using PCR-mediated mutagenesis to generate pLR1287.

387

388 **Immunoblotting**

389 Immunoblots were performed as previously described (Hickman and Rusche 2010). Cells were  
390 grown to an OD<sub>600</sub> of ~1.0, and fixed with a final concentration of 10% TCA. For lysis, 40 OD equivalents  
391 of fixed cells were vortexed 5 min in the presence of silica beads (0.5 mm dia. #11079105z, BioSpec  
392 Products) in 40 µl lysis buffer (10 mM HEPES pH 7.9, 150 mM KCl, 1.5 mM MgCl<sub>2</sub>, 0.5 mM DTT, 10%  
393 glycerol, 5 µg/ml chymostatin, 2 µg/ml pepstatin A, 156 µg/ml benzamidine, 35.2 µg/ml TPCK, 174 µg/ml  
394 PMSF, and 1× Complete Protease Inhibitor (Roche)). Proteins were denatured by the addition of 1/3 volume  
395 3X sample buffer (30% glycerol, 15% β-mercaptoethanol, 6% SDS, 200 mM Tris pH 6.8, 0.08 mg/ml  
396 bromophenol blue) and incubation at 95° for 5 min. Finally, samples were clarified by centrifugation.  
397 Aliquots (10 µl) of protein extract were resolved on a 7.5% acrylamide gel, transferred to membrane  
398 (Amersham 45004008), and probed to detect Orc1 protein (anti-MYC, Millipore 06-549), Orc2 or Orc4  
399 proteins (anti-V5, Millipore AB3792) or Pgk1 (ab113687, Abcam) as a loading control.

400

401 **Transformation frequency and plasmid loss assay**

402 For the transformation frequency assay, *T. delbrueckii* cells were transformed with 5 ng plasmid  
403 and plated on selective medium (YPD + 400 µg/mL hygromycin). Three replicate transformations were  
404 performed, and colony images were taken after two days growth at 30°C. The colony areas were determined  
405 for all the colonies from three replicate transformation plates using Image J and then averaged (Schneider,  
406 et al. 2012).

407 For the plasmid loss assay, three single colonies were used to inoculate 5 ml YPD + hygromycin  
408 and grown for 22 hours to an OD<sub>600</sub> of approximately 13. Aliquots of each culture were plated onto three  
409 selective (YPD + hygromycin) and nonselective (YPD) plates to determine the fraction of cells resistant to  
410 hygromycin and hence containing the plasmid. The culture was also diluted to OD<sub>600</sub> = 0.0003 in

411 nonselective (YPD) medium and grown for 30 hours to an OD<sub>600</sub> of approximately 13. The fraction of cells  
412 containing plasmid was then determined as described above.

413

#### 414 **Chromatin immunoprecipitation and sequencing**

415 Chromatin immunoprecipitation was performed as previously described (Rusche and Rine 2001).  
416 Cells were grown in YPD at 30°C, harvested at an OD<sub>600</sub> of ~1, and cross-linked for 1 hour in 1%  
417 formaldehyde. For immunoprecipitation, 4 µl of anti MYC antibody (Millipore 06-549) or anti V5 antibody  
418 (Millipore AB3792) were used. The immunoprecipitation was conducted with 10 µL of Protein A agarose  
419 beads in the absence of BSA and salmon sperm DNA. Library preparation (Takara Bio SMARTer ThruPlex  
420 DNA seq kit) and sample barcoding was done at the Next-Generation Sequencing facility at University at  
421 Buffalo. The samples were then sequenced on an Illumina 1.9 sequencer using 76 bp single-end sequencing  
422 for Orc1-3XMYC (LRY3204 and LRY3211) and 151 bp paired-end sequencing for Orc2-V5 and Orc4-V5  
423 (LRY3142, LRY3143, LRY3138 and LRY3139).

424

#### 425 **Bioinformatics analysis pipeline**

426 Prior to sequence alignment, the paired-end sequence reads were processed to remove 3' adapter  
427 sequences (" -a AGATCGGAAGAGCACACGTCTGAAGTCAGTCA -A AGATCGGAAGAGCGTCGTAGGGAAA  
428 GAGTGT") using Cutadapt/2.10 (Martin 2011) with the parameters "--nextseq-trim=20, -m 10". Trimmed  
429 paired-end reads and raw single-end reads were aligned to the *T. delbrueckii* genome (CBS1146  
430 (GCA\_000243375.1)) (Gordon, et al. 2011) using Bowtie2/2.3.4.1 (Langmead, et al. 2009). Samtools/1.9  
431 (Li, et al. 2009) was used to convert .sam output files from Bowtie2/2.3.4.1 to .bam, -sorted.bam and index  
432 files. To identify ORC binding sites, Model-based Analysis of ChIP-Seq, MACS2/2.2.7.1 (Zhang, et al.  
433 2008) was used to call peaks using one million randomly selected high quality reads with mock IP as control  
434 for Orc2 and Orc4 and genomic input as control for Orc1 samples; For all samples, --nomodel was used, -  
435 -extsize 200 was used for single-end reads only, and -f BEDPE was used for paired-end reads only. To  
436 determine intersecting peaks for Orc1, Orc2, and Orc4, Bedtools/2.23.0 (Quinlan and Hall 2010) was used

437 with the parameters “-f 0.4, -r” which requires at least 40% overlap among all peaks. Finally, to determine  
438 the ORC binding motif, MEME Suite 5.3.0 (Multiple Em for Motif Elicitation) (Bailey, et al. 2009) was  
439 used with the 190 ORC-binding sites as input.

440 To compare the ORC-binding motifs of various species, the coordinates of replication origins were  
441 retrieved from published literature for *S. cerevisiae* (Belsky, et al. 2015), *K. lactis* (Liachko, et al. 2010),  
442 *C. glabrata* (Descorps-Declère, et al. 2015), *L. kluyveri* (Liachko, et al. 2011) and *L. waltii* (Di Rienzi, et  
443 al. 2012). Reference genomes for *S. cerevisiae* (GCF\_000146045.2), *K. lactis* (GCF\_000002515.2), *C.*  
444 *glabrata* (GCF\_000002545.3), and *L. kluyveri* (GCA\_000149225.1) were downloaded from NCBI. The  
445 reference genome for *L. waltii* was provided by M. K. Raghuraman (Di Rienzi, et al. 2009). MEME (Bailey,  
446 et al. 2009) was used to search for consensus motifs in 269 *S. cerevisiae*, 124 *K. lactis*, 275 *C. glabrata*, 84  
447 *L. kluyveri* and 194 *L. waltii* sequences. The search assumed the motif is present zero or once per sequence  
448 (the ZOOPS model) and enriched over the background. A first order Markov model of the background was  
449 built for *T. delbrueckii*, a second order Markov model of the background was built for *S. cerevisiae* and *L.*  
450 *waltii*, a fourth order Markov model of the background was built for *K. lactis* and *L. kluyveri*, and a zero  
451 order Markov model of the background was built for *C. glabrata*. A 33 bp motif was specified for *S.*  
452 *cerevisiae*, *C. glabrata*, *L. waltii*, and *T. delbrueckii*, a 9 bp motif was specified for *L. kluyveri*, and a 50 bp  
453 motif was specified for *K. lactis*.

454 Aggregate plot and heat maps for ChIP-Seq signals for Orc1, Orc2 and Orc4 were generated using  
455 DeepTools/3.5.0 (Ramirez, et al. 2014). For this analysis, .bed files of two replicates for each ORC subunit  
456 were combined using MACS/2.2.7.1. DeepTools/3.5.0 ‘computeMatrix reference-point’ was used to  
457 calculate scores per genome region using the parameters “--sortRegions no --binSize 10”. For both  
458 aggregate plot and heat map the ChIP-Seq signals from the three ORC subunits were centered around the  
459 33 bp motif generated from MEME and extended 1 kb base pairs upstream and downstream of the motif.

460

461 **Data availability**

462 The data underlying this article, including raw Illumina data for Orc1/2/4 ChIP-sequencing were  
463 uploaded at the NCBI GEO database (Accession number: GSE165127).

464

## 465 Acknowledgements

466 We thank Aigerim Nuganova for assistance in making plasmids, Michael Buck for suggestions on ChIP-  
467 seq data analysis, Jasper Rine and Aisha Ellahi for strains and plasmids, M. K. Raghuraman for providing  
468 the *L. waltii* genome assembly, Derek Taylor for assistance on the phylogenetic tree construction and  
469 members of the Rusche lab for suggestions and support. Bioinformatic analysis was supported by the Center  
470 for Computational Research at the University at Buffalo (<http://hdl.handle.net/10477/79221>). This work  
471 was supported by the National Science Foundation (MCB 1615367) and the Mark Diamond Research Fund  
472 of the Graduate Student Association at the University at Buffalo, the State University of New York.

473

## 474 References

475 Agier N, et al. 2018. The evolution of the temporal program of genome replication. *Nature Communications* 9: 2199. doi: 10.1038/s41467-018-04628-4  
476  
477 Aguileta G, et al. 2008. Assessing the performance of single-copy genes for recovering robust  
478 phylogenies. *Syst Biol* 57: 613-627. doi: 10.1080/10635150802306527  
479 Bailey TL, et al. 2009. MEME SUITE: tools for motif discovery and searching. *Nucleic Acids Res* 37: W202-  
480 208. doi: 10.1093/nar/gkp335  
481 Bell SP, Stillman B 1992. ATP-dependent recognition of eukaryotic origins of DNA replication by a  
482 multiprotein complex. *Nature* 357: 128-134. doi: 10.1038/357128a0  
483 Belsky JA, MacAlpine HK, Lubelsky Y, Hartemink AJ, MacAlpine DM 2015. Genome-wide chromatin  
484 footprinting reveals changes in replication origin architecture induced by pre-RC assembly. *Genes Dev*  
485 29: 212-224. doi: 10.1101/gad.247924.114  
486 Brand AH, Breeden L, Abraham J, Sternglanz R, Nasmyth K 1985. Characterization of a "silencer" in yeast:  
487 a DNA sequence with properties opposite to those of a transcriptional enhancer. *Cell* 41: 41-48. doi:  
488 10.1016/0092-8674(85)90059-5  
489 Byrne KP, Wolfe KH 2005. The Yeast Gene Order Browser: combining curated homology and syntetic  
490 context reveals gene fate in polyploid species. *Genome Res* 15: 1456-1461. doi: 10.1101/gr.3672305  
491 Chan CS, Tye BK 1980. Autonomously replicating sequences in *Saccharomyces cerevisiae*. *Proceedings of*  
492 *the National Academy of Sciences* 77: 6329-6333. doi: 10.1073/pnas.77.11.6329  
493 Clyne RK, Kelly TJ 1997. Identification of autonomously replicating sequence (ARS) elements in  
494 eukaryotic cells. *Methods* 13: 221-233. doi: 10.1006/meth.1997.0522

495 Dai J, Chuang R-Y, Kelly TJ 2005. DNA replication origins in the *Schizosaccharomyces pombe* genome.  
496 Proceedings of the National Academy of Sciences of the United States of America 102: 337-342. doi:  
497 10.1073/pnas.0408811102

498 Descorps-Declère S, et al. 2015. Genome-wide replication landscape of *Candida glabrata*. BMC Biology  
499 13: 69. doi: 10.1186/s12915-015-0177-6

500 Di Rienzi SC, Collingwood D, Raghuraman MK, Brewer BJ 2009. Fragile genomic sites are associated with  
501 origins of replication. Genome Biol Evol 1: 350-363. doi: 10.1093/gbe/evp034

502 Di Rienzi SC, et al. 2012. Maintaining replication origins in the face of genomic change. Genome Res 22:  
503 1940-1952. doi: 10.1101/gr.138248.112

504 Eaton ML, Galani K, Kang S, Bell SP, MacAlpine DM 2010. Conserved nucleosome positioning defines  
505 replication origins. Genes Dev 24: 748-753. doi: 10.1101/gad.1913210

506 Ellahi A, Rine J 2016. Evolution and Functional Trajectory of Sir1 in Gene Silencing. Mol Cell Biol 36:  
507 1164-1179. doi: 10.1128/mcb.01013-15

508 Friedman KL, Brewer BJ, Fangman WL 1997. Replication profile of *Saccharomyces cerevisiae*  
509 chromosome VI. Genes to cells : devoted to molecular & cellular mechanisms 2: 667-678. doi:  
510 10.1046/j.1365-2443.1997.1520350.x

511 Funakoshi M, Hochstrasser M 2009. Small epitope-linker modules for PCR-based C-terminal tagging in  
512 *Saccharomyces cerevisiae*. Yeast 26: 185-192. doi: 10.1002/yea.1658

513 Gomez-Angulo J, et al. 2015. Genome Sequence of *Torulaspora delbrueckii* NRRL Y-50541, Isolated from  
514 Mezcal Fermentation. Genome Announc 3. doi: 10.1128/genomeA.00438-15

515 Gordon JL, et al. 2011. Evolutionary erosion of yeast sex chromosomes by mating-type switching  
516 accidents. Proc Natl Acad Sci U S A 108: 20024-20029. doi: 10.1073/pnas.1112808108

517 Gouy M, Guindon S, Gascuel O 2010. SeaView version 4: A multiplatform graphical user interface for  
518 sequence alignment and phylogenetic tree building. Mol Biol Evol 27: 221-224. doi:  
519 10.1093/molbev/msp259

520 Hickman MA, Rusche LN 2009. The Sir2-Sum1 Complex Represses Transcription Using Both Promoter-  
521 Specific and Long-Range Mechanisms to Regulate Cell Identity and Sexual Cycle in the Yeast  
522 *Kluyveromyces lactis*. PLoS Genet 5: e1000710. doi: 10.1371/journal.pgen.1000710

523 Hickman MA, Rusche LN 2010. Transcriptional silencing functions of the yeast protein Orc1/Sir3  
524 subfunctionalized after gene duplication. Proc Natl Acad Sci U S A 107: 19384-19389. doi:  
525 10.1073/pnas.1006436107

526 Hoang DT, Chernomor O, von Haeseler A, Minh BQ, Vinh LS 2018. UFBoot2: Improving the Ultrafast  
527 Bootstrap Approximation. Mol Biol Evol 35: 518-522. doi: 10.1093/molbev/msx281

528 Hsiao CL, Carbon J 1979. High-frequency transformation of yeast by plasmids containing the cloned  
529 yeast ARG4 gene. Proc Natl Acad Sci U S A 76: 3829-3833. doi: 10.1073/pnas.76.8.3829

530 Hu Y, et al. 2020. Evolution of DNA replication origin specification and gene silencing mechanisms. Nat  
531 Commun 11: 5175. doi: 10.1038/s41467-020-18964-x

532 Katoh K, Standley DM 2013. MAFFT multiple sequence alignment software version 7: improvements in  
533 performance and usability. Mol Biol Evol 30: 772-780. doi: 10.1093/molbev/mst010

534 Koren A, et al. 2011. Correction: Epigenetically-Inherited Centromere and Neocentromere DNA  
535 Replicates Earliest in S-Phase. PLoS Genet 7: 10.1371/annotation/d1374e1378b1374eb-2385-  
536 1374a1346-1938e-1319bbae1374fcf1389. doi: 10.1371/annotation/d4e8b4eb-2385-4a46-938e-  
537 19bbae4fcf89

538 Langmead B, Trapnell C, Pop M, Salzberg SL 2009. Ultrafast and memory-efficient alignment of short  
539 DNA sequences to the human genome. Genome Biology 10: R25. doi: 10.1186/gb-2009-10-3-r25

540 Lee DG, Bell SP 1997. Architecture of the yeast origin recognition complex bound to origins of DNA  
541 replication. Mol Cell Biol 17: 7159-7168. doi: 10.1128/mcb.17.12.7159

542 Li H, et al. 2009. The Sequence Alignment/Map format and SAMtools. *Bioinformatics* 25: 2078-2079. doi:  
543 10.1093/bioinformatics/btp352

544 Liachko I, et al. 2010. A comprehensive genome-wide map of autonomously replicating sequences in a  
545 naive genome. *PLoS Genet* 6: e1000946. doi: 10.1371/journal.pgen.1000946

546 Liachko I, et al. 2011. Novel features of ARS selection in budding yeast *Lachancea kluyveri*. *BMC*  
547 *Genomics* 12: 633. doi: 10.1186/1471-2164-12-633

548 Lipford JR, Bell SP 2001. Nucleosomes positioned by ORC facilitate the initiation of DNA replication. *Mol*  
549 *Cell* 7: 21-30. doi: 10.1016/s1097-2765(01)00151-4

550 Maguire SL, et al. 2013. Comparative genome analysis and gene finding in *Candida* species using CGOB.  
551 *Mol Biol Evol* 30: 1281-1291. doi: 10.1093/molbev/mst042

552 Marahrens Y, Stillman B 1992. A yeast chromosomal origin of DNA replication defined by multiple  
553 functional elements. *Science* 255: 817-823. doi: 10.1126/science.1536007

554 Marcet-Houben M, Gabaldon T 2015. Beyond the Whole-Genome Duplication: Phylogenetic Evidence  
555 for an Ancient Interspecies Hybridization in the Baker's Yeast Lineage. *PLoS Biol* 13: e1002220. doi:  
556 10.1371/journal.pbio.1002220

557 Martin M 2011. Cutadapt removes adapter sequences from high-throughput sequencing reads. 2011 17:  
558 3. doi: 10.14806/ej.17.1.200

559 McCarroll RM, Fangman WL 1988. Time of replication of yeast centromeres and telomeres. *Cell* 54: 505-  
560 513. doi: [https://doi.org/10.1016/0092-8674\(88\)90072-4](https://doi.org/10.1016/0092-8674(88)90072-4)

561 Mei Q, et al. 2017. Regulation of DNA replication-coupled histone gene expression. *Oncotarget* 8:  
562 95005-95022. doi: 10.18632/oncotarget.21887

563 Müller CA, Nieduszynski CA 2012. Conservation of replication timing reveals global and local regulation  
564 of replication origin activity. *Genome Res* 22: 1953-1962. doi: 10.1101/gr.139477.112

565 Müller CA, Nieduszynski CA 2017. DNA replication timing influences gene expression level. *The Journal*  
566 *of cell biology* 216: 1907-1914. doi: 10.1083/jcb.201701061

567 Nieduszynski CA, Hiraga S-i, Ak P, Benham CJ, Donaldson AD 2007. OriDB: a DNA replication origin  
568 database. *Nucleic Acids Res* 35: D40-D46. doi: 10.1093/nar/gkl758

569 Patel PK, Arcangioli B, Baker SP, Bensimon A, Rhind N 2006. DNA replication origins fire stochastically in  
570 fission yeast. *Mol Biol Cell* 17: 308-316. doi: 10.1091/mbc.e05-07-0657

571 Quinlan AR, Hall IM 2010. BEDTools: a flexible suite of utilities for comparing genomic features.  
572 *Bioinformatics* 26: 841-842. doi: 10.1093/bioinformatics/btq033

573 Raghuraman MK, et al. 2001. Replication dynamics of the yeast genome. *Science* 294: 115-121. doi:  
574 10.1126/science.294.5540.115

575 Ramirez F, Dündar F, Peter S, Grüning B, Manke T 2014. DeepTools: A flexible platform for exploring  
576 deep-sequencing data. *Nucleic Acids Res* 42. doi: 10.1093/nar/gku365

577 Rusche LN, Rine J 2001. Conversion of a gene-specific repressor to a regional silencer. *Genes Dev* 15:  
578 955-967. doi: 10.1101/gad.873601

579 Schneider CA, Rasband WS, Eliceiri KW 2012. NIH Image to ImageJ: 25 years of image analysis. *Nature*  
580 *Methods* 9: 671-675. doi: 10.1038/nmeth.2089

581 Segurado M, de Luis A, Antequera F 2003. Genome-wide distribution of DNA replication origins at A+T-  
582 rich islands in *Schizosaccharomyces pombe*. *EMBO Rep* 4: 1048-1053. doi:  
583 10.1038/sj.embo.7400008

584 Shen XX, et al. 2018. Tempo and Mode of Genome Evolution in the Budding Yeast Subphylum. *Cell* 175:  
585 1533-1545.e1520. doi: 10.1016/j.cell.2018.10.023

586 Sikorski RS, Hieter P 1989. A system of shuttle vectors and yeast host strains designed for efficient  
587 manipulation of DNA in *Saccharomyces cerevisiae*. *Genetics* 122: 19-27.

588 Struhl K, Stinchcomb DT, Scherer S, Davis RW 1979. High-frequency transformation of yeast:  
589 autonomous replication of hybrid DNA molecules. Proc Natl Acad Sci U S A 76: 1035-1039. doi:  
590 10.1073/pnas.76.3.1035  
591 Theis JF, Newlon CS 1997. The ARS309 chromosomal replicator of *Saccharomyces cerevisiae* depends on  
592 an exceptional ARS consensus sequence. Proc Natl Acad Sci U S A 94: 10786-10791. doi:  
593 10.1073/pnas.94.20.10786  
594 Theis JF, Yang C, Schaefer CB, Newlon CS 1999. DNA sequence and functional analysis of homologous  
595 ARS elements of *Saccharomyces cerevisiae* and *S. carlsbergensis*. Genetics 152: 943-952.  
596 Trifinopoulos J, Nguyen LT, von Haeseler A, Minh BQ 2016. W-IQ-TREE: a fast online phylogenetic tool  
597 for maximum likelihood analysis. Nucleic Acids Res 44: W232-235. doi: 10.1093/nar/gkw256  
598 Xu W, Aparicio JG, Aparicio OM, Tavaré S 2006. Genome-wide mapping of ORC and Mcm2p binding sites  
599 on tiling arrays and identification of essential ARS consensus sequences in *S. cerevisiae*. BMC Genomics  
600 7: 276. doi: 10.1186/1471-2164-7-276  
601 Yuan Z, et al. 2017. Structural basis of Mcm2-7 replicative helicase loading by ORC-Cdc6 and Cdt1.  
602 Nature structural & molecular biology 24: 316-324. doi: 10.1038/nsmb.3372  
603 Zhang Y, et al. 2008. Model-based Analysis of ChIP-Seq (MACS). Genome Biology 9: R137. doi:  
604 10.1186/gb-2008-9-9-r137  
605 Zou L, Stillman B 2000. Assembly of a complex containing Cdc45p, replication protein A, and Mcm2p at  
606 replication origins controlled by S-phase cyclin-dependent kinases and Cdc7p-Dbf4p kinase. Mol Cell Biol  
607 20: 3086-3096. doi: 10.1128/mcb.20.9.3086-3096.2000

608

609 Figures and Legends

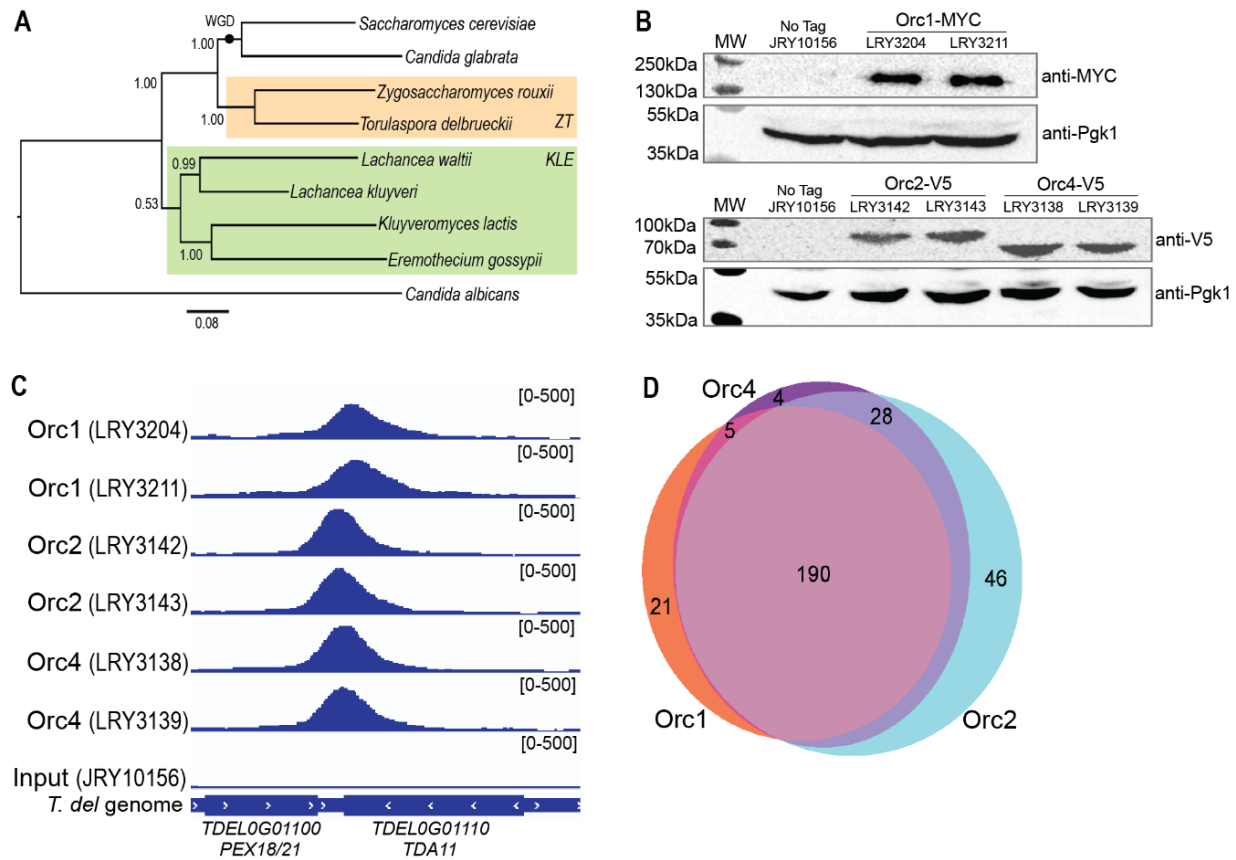


**Fig. 1. Identification of Orc1, Orc2 and Orc4 binding sites in *T. delbrueckii*.** **(A)** Evolutionary relationship of the species discussed in the paper. A species tree was built using a maximum likelihood approach on a concatenated alignment of 10 single copy genes. Node support values (aLRT, approximate likelihood ratio test) are shown. WGD denotes the whole genome duplication (WGD). ZT denotes the *Zygosaccharomyces* and *Torulaspora* clade (tan box), and KLE denotes the *Kluyveromyces*, *Lachancea*, and *Eremothecium* clade (green box). **(B)** Immunoblot of tagged ORC subunits TdOrc1-3XMYC (LRY3204, LRY3211), TdOrc2-V5 (LRY3142, LRY3143) and TdOrc4-V5 (LRY3138, LRY3139). The untagged parent strain (JRY10156) was included as a control. Endogenous 3-phosphoglycerate kinase (Pgk1) was detected as a loading control. **(C)** A representative ORC binding site on Chromosome VII, ARS\_VII\_228, is depicted. Each line represents the read depth of sequences generated by ChIP-Seq from

one tagged ORC strain. The bottom line shows the positions of genes flanking the ORC binding site. **(D)** Venn diagram indicating the overlap between 216 Orc1 binding sites (coral), 264 Orc2 binding sites (blue), and 227 Orc4 binding sites (purple).

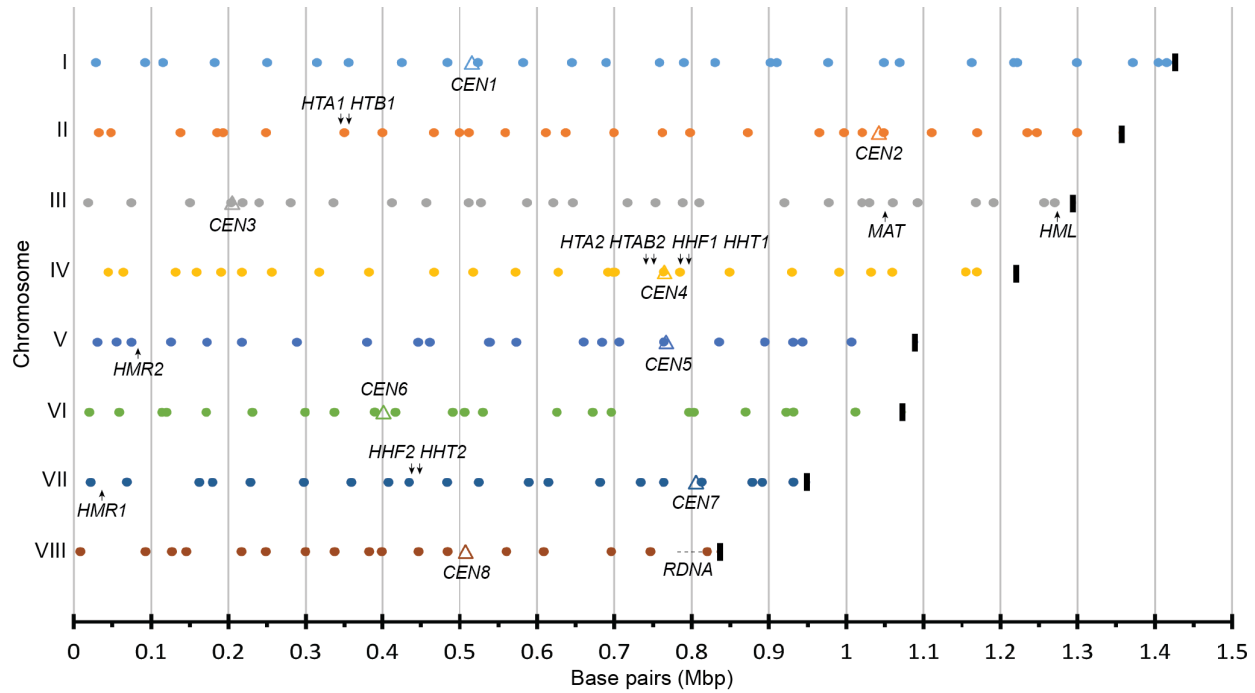
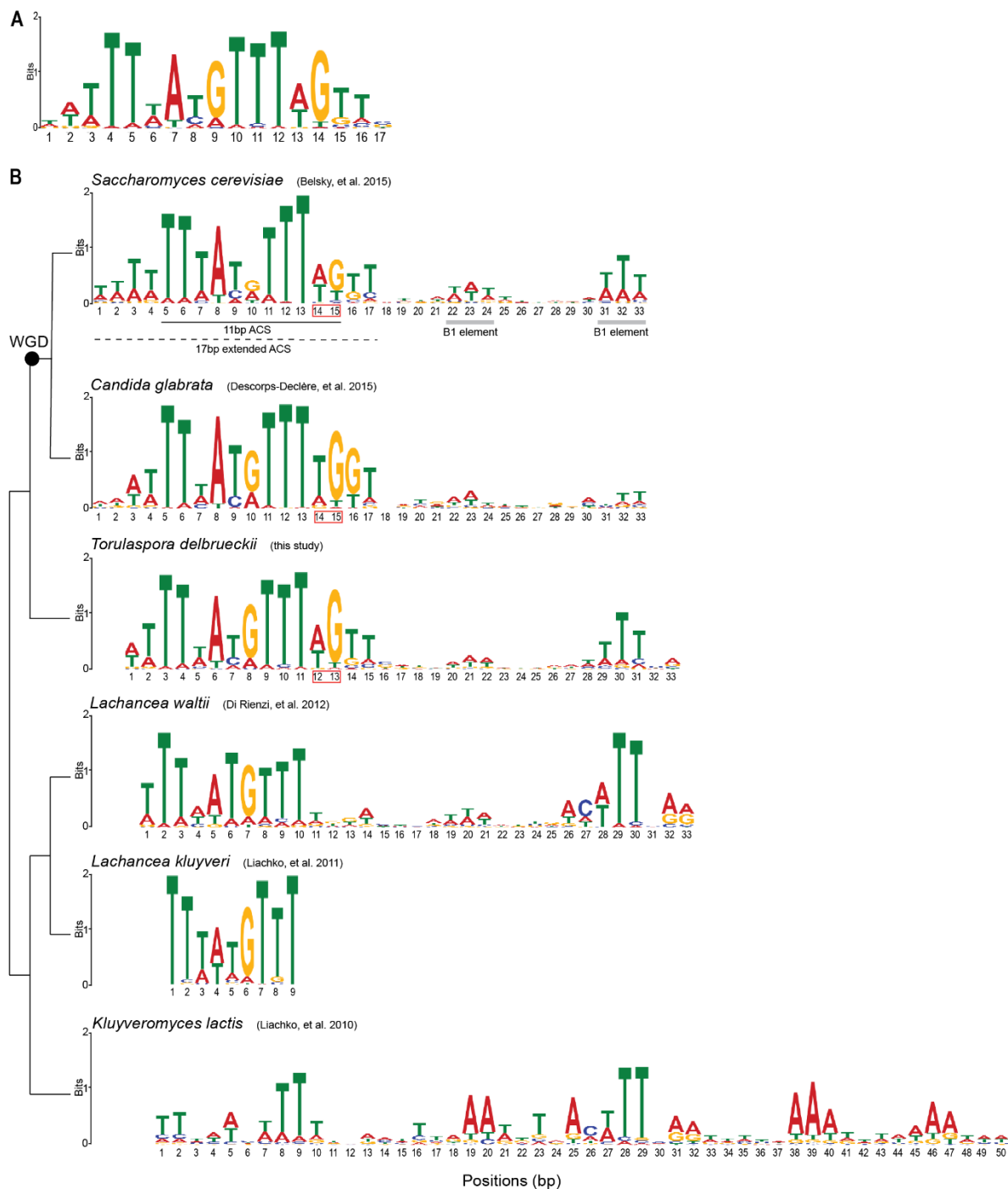


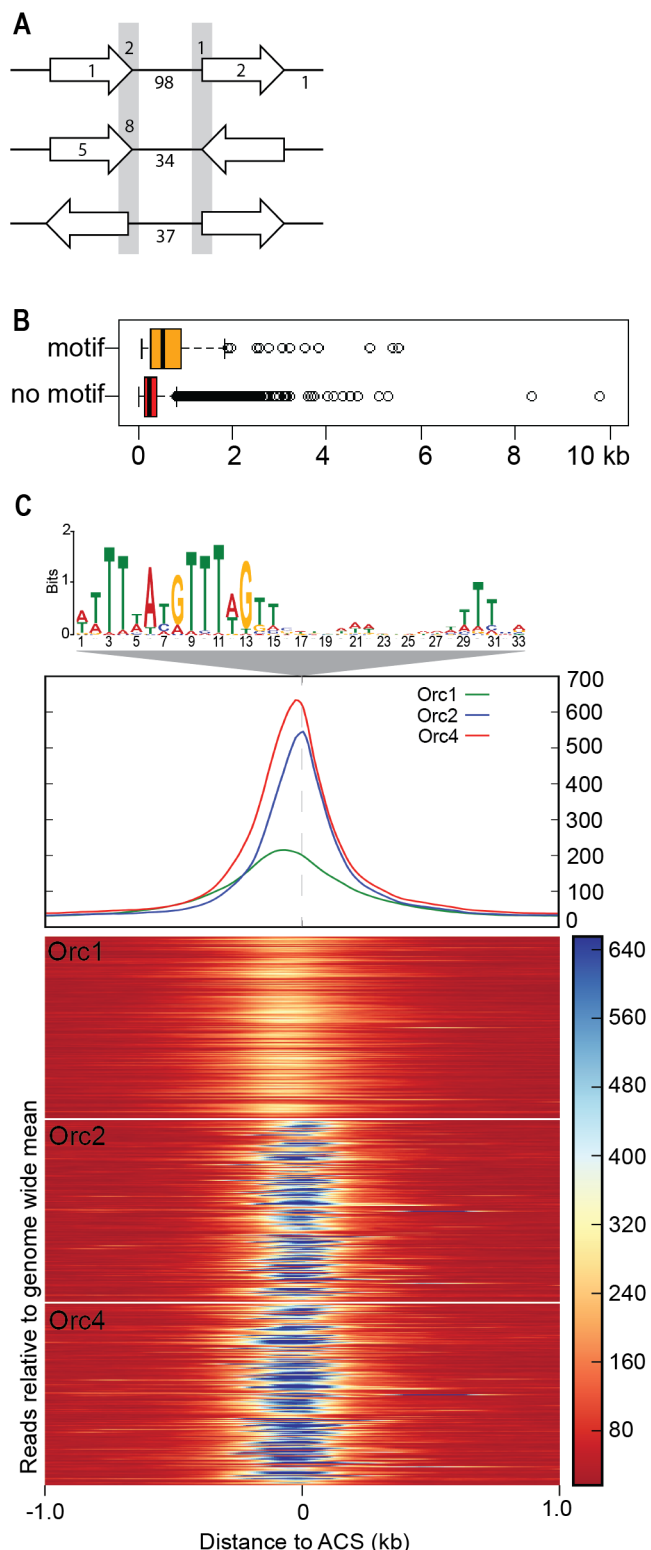
**Fig. 2. Genome-wide distribution of ORC binding sites.** Dots represent the 190 ORC binding sites on each of the eight *T. delbrueckii* chromosomes. Thick vertical black lines indicate the right end of each chromosome, and  $\Delta$  indicates the centromere. The histone genes, *HTA*, *HTB*, *HHF*, and *HHT*, are indicated with black arrows. The mating type loci, *MAT*, *HML*, and *HMR*, and the rDNA repeat locus (dashed line) are genomic landmarks shown for reference. Every major unit on the scale represents 100,000 base pairs.



c

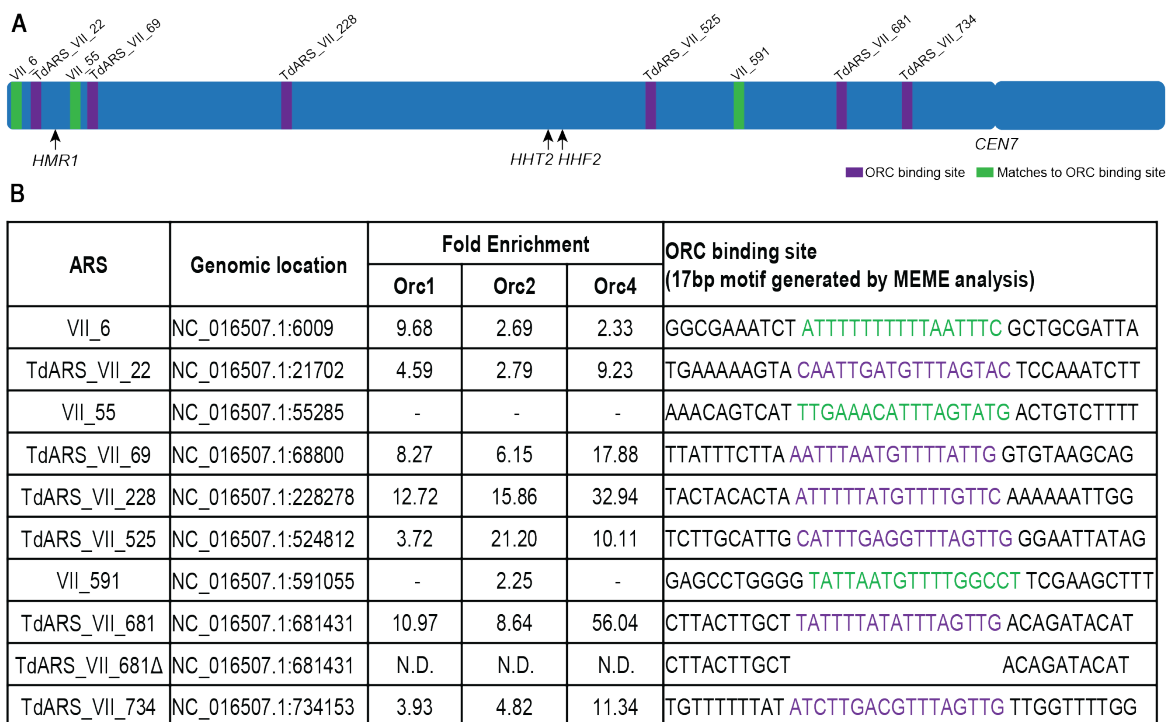
		Orc4 insertion a-helix	
<i>S.cerevisiae</i> _Orc4	455	DVKNVWENLVQLDFTEKSAGVLRDNDAAF <del>YASNYQFQGTMIPFDLRLSYQM</del>	506
<i>C.glabrata</i> _Orc4	465	DIKNVWESLSLGFLAEKSDVGLRESAMAV <del>YASNYQLQGNALPYDRLRVYQM</del>	516
<i>T.delbrueckii</i> _Orc4	497	DVKNVWETLINLNFLTEKSAGVLR <del>RESAIAFVYASNYQLQGTTIPFDLRLYQT</del>	548
<i>L.waltii</i> _Orc4	425	DVKNVWENLIDLD <del>FITEKG</del> SVGLRASALAAFMASNYQ <del>STGTIIPFDLRLTYQM</del>	476
<i>L.kluyveri</i> _Orc4	597	DIKNVWENI <del>ELN</del> FILEK <del>GAV</del> GLRVSAQAA <del>FQAS</del> NYHT <del>GTT</del> IPFDLRLMYQL	648
<i>K.lactis</i> _Orc4	474	DMKNVWENL <del>AN</del> QEL <del>ITERGA</del> ISVRFTEDSAIQ <del>SAN</del> NSSTM <del>KAP</del> FDLRLTYQM	525
	*****	*****	*****

610 **Fig. 3. Comparison of sequence motifs associated with *T. delbrueckii* ORC binding sites and other**  
611 **known origins of replication. (A)** A 17bp motif was found in 187 of 190 *T. delbrueckii* ORC binding sites  
612 by MEME (Bailey, et al. 2009) when the motif length was not specified. **(B)** A longer motif was found in  
613 189 of 190 predicted *T. delbrueckii* ORC binding sites when the motif length was fixed to 33. This motif is  
614 compared to known motifs from *S. cerevisiae* (Belsky, et al. 2015), *C. glabrata* (Descorps-Declère, et al.  
615 2015), *L. kluyveri* (Liachko, et al. 2011), *K. lactis* (Liachko, et al. 2011) and *L. waltii* (Di Rienzi, et al.  
616 2012). The cladogram representing the relationships of the species (Marcet-Houben and Gabaldon 2015) is  
617 not to scale. WGD denotes the whole genome duplication. For *S. cerevisiae*, the 11 bp ACS is underlined  
618 by a solid black line, the extended ACS /A element is underlined by a black dotted line, and the B1 elements  
619 are underlined by gray boxes. **(C)** Alignment of a portion of Orc4 from the same species. The DNA-binding  
620 alpha helix is highlighted grey, and the tyrosine (Y) that contacts nucleotides 14 and 15 in *S. cerevisiae* and  
621 likely nucleotides 12 and 13 in *T. delbrueckii* (red boxed in 3B) (Hu, et al. 2020) is highlighted red.



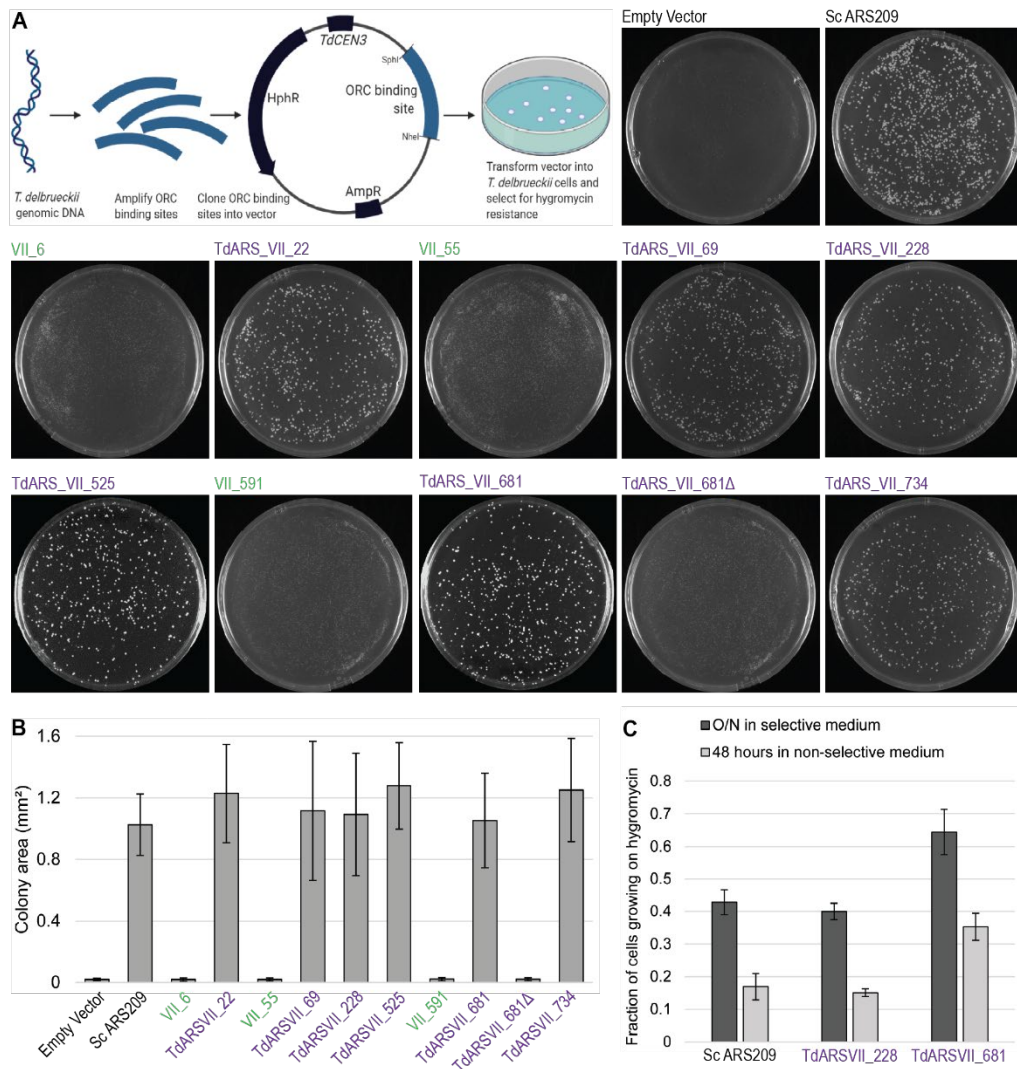
622 **Fig. 4. The ORC-binding motif is preferentially located between genes and coincides with the peak of**  
 623 **ORC binding. (A)** Position and number of ORC binding motifs relative to the flanking genes. The arrows

624 indicate the transcription direction of the genes. Motifs included within the vertical grey bars span the  
 625 junction between the gene and the intergenic region. One ORC binding motif occurs between the last gene  
 626 and the end of the chromosome (top line). **(B)** Box and whisker plot representing the sizes (kb) of intergenic  
 627 regions with and without an ORC binding site. Each box shows the 25<sup>th</sup>, 50<sup>th</sup> and 75<sup>th</sup> percentile. The vertical  
 628 line in each box represents the median size. The whiskers show 10<sup>th</sup> and 90<sup>th</sup> percentiles. **(C)** Aggregate  
 629 plot (middle) and heat maps (bottom) of ChIP-Seq signals for Orc1, Orc2 and Orc4 are shown centered on  
 630 the 33 bp motif (top) generated using MEME. Data for each binding site is oriented with the ACS to the  
 631 left and B1 element to the right. The y-axis for the aggregate plot and heat maps represents average read  
 632 depth of sequences generated by ChIP-Seq. The x axis represents ChIP-Seq signals across 1 kb upstream  
 633 and downstream of the 33 bp motif.



634 **Fig. 5. ORC-binding sites on chromosome VII tested for ARS activity. (A)** Diagram of *T. delbrueckii*  
 635 chromosome VII. Purple bars represent the six (out of 21) ORC binding sites on chromosome VII that  
 636 were tested for ARS activity. Green bars represent three sites with matches to the motif but low or no

637 enrichment of ORC subunits. The black arrows indicate the position of the cryptic mating type locus,  
 638 *HMRI*, and the histone genes, *HHT2* and *HHF2*. **(B)** For the nine sites that were tested, the table summarizes  
 639 the genomic location, fold enrichment of Orc1, Orc2, and Orc4, and the match to the 17 bp consensus  
 640 sequence identified by MEME (proposed ACS; purple).



641 **Fig. 6. ORC binding sites act as autonomously replicating sequences (ARSs) on plasmids. (A)** To test  
 642 for ARS activity, a hygromycin-sensitive *T. delbrueckii* strain (JRY10156) was transformed with plasmids  
 643 bearing various ORC binding sites and a hygromycin-resistance gene. Hygromycin-resistant colonies were  
 644 imaged after two days. Controls were plasmids lacking an ARS (empty vector) and bearing *ScARS209*, a

645 *S. cerevisiae* origin known to function in *T. delbrueckii*. **(B)** The average area of the colonies shown in  
646 panel A was calculated using Image J (Schneider, et al. 2012). Error bars represent standard deviations  
647 between three replicate experiments. **(C)** Plasmid loss assays were performed on TdARS\_VII\_228,  
648 TdARS\_VII\_681, and ScARS209. The fraction of cells able to grow on hygromycin, and therefore  
649 containing plasmids with the hygromycin-resistance gene, was determined before and after growth in non-  
650 selective medium (YPD) for 30 hours. Error bars represent the standard error of the mean of three replicate  
651 experiments.